Int J Appl Earth Obs Geoinformation 93 (2020) 102207

Contents lists available at ScienceDirect

Int J Appl Earth Obs Geoinformation

journal homepage: www.elsevier.com/locate/jag

Sentinel-2 time series based optimal features and time window for mapping invasive Australian native *Acacia* species in KwaZulu Natal, South Africa

Cecilia Masemola[a,b,*], Moses Azong Cho[d,c], Abel Ramoelo[e,f]

[a] *Discipline of Geography, School of Agricultural, Earth and Environmental Sciences, University of KwaZulu-Natal, Private Bag X01, Scottsville, Pietermaritzburg, 3209, South Africa*
[b] *College of Agriculture and Environmental Science, University of South Africa, Pretoria, South Africa*
[c] *Earth Observation Research Group, Natural Resources and Environment, Council for Scientific and Industrial Research, Pretoria, South Africa*
[d] *Forest Science Postgraduate Programme, Department of Plant and Soil Science, University of Pretoria, South Africa*
[e] *Conservation Services, South African National Parks (SANParks), P.O. Box 787, Pretoria, 0001, South Africa*
[f] *Vulnerability Assessment Centre, University of Limpopo, Sovenga, South Africa*

A B S T R A C T

The spread of invasive Australia native *Acacia* tree species threatens biodiversity and adversely affecting on vegetative structure and function, including plant community composition, quantity and quality worldwide. It is essential to provide researchers and land managers for biological invasion science and management with accurate information of the distribution of invasive alien species and their dynamics. Remotely sensed data that reveal spatial distribution of the earth's surface features/objects provide great potential for this purpose. Consistent satellite monitoring of alien invasive plants is often difficult because of lack of sufficient spectral contrast between them and co-occurring plants species. Time series analysis of spectral properties of the species can reveal timing of their variations among adjacent species. This information can improve accuracy of invasive species discrimination and mapping using remote sensing data at large scale. We sought to identify and better understand the optimal time window and key spectral features sufficient to detect invasive *Acacia* trees in heterogeneous forested landscape in South Africa. We explored one-year (January to December 2018) time series spectral bands and vegetation indices derived from optical Copernicus Sentinel-2 data. The attributes correspond to geographical information of invasive *Acacia* and native species recorded during a field survey undertaken from 21 February to 25 February 2018 over Kwa-Zulu Natal grasslands landscape, in South Africa. The results showed comparable separability prospects between times series of spectral bands and that of vegetation indices.

Substantial differences between *Acacia species* and native species were observed from spectral indices and spectral bands which are sensitive to Leaf Area Index, canopy chlorophyll and nitrogen concentrations. The results further revealed spectral differences between Acacia species and co-occurring native vegetation in April (senescence for deciduous plants), June-July (dry season), September (peak flowering period of *Acacia spp*) and December (leaf green-up) with vegetation indices (overall accuracy > 80 %). While spectral bands showed the beginning of the growing season (November–January) and peak vegetation productivity (February-March) as the optimal seasons or dates for image acquisition for discriminating *Acacias* from its co-occurring native species (overall accuracy > 80 %). In general, the use of Sentinel-2 time series spectral bands and vegetation indices has increased our understanding of Australian *Acacias* spectral dynamics, and proved that the sentinel-2 data is useful for characterization and monitoring Acacias over a large scale. Our results and approach could assist in deriving detailed geographic information of the species and assessment of a spread invasive plant species and severity of invasion.

1. Introduction

Invasive alien plants (IAP) are the cause of global biodiversity loss (Pyšek et al., 2012). Biodiversity loss has consequences for native species richness, diversity and composition as well as ecosystem functioning (Cardinale et al., 2012). South Africa is no exception; the country is invaded by mainly Australian Native *Acacias* (*Acacia mearnsii, Acacia saligna, Acacia longifolia and Acacia dealbata*) (Marchante et al., 2015; Maitre et al., 2011; de Sá et al., 2018; van Wilgen and Wilson, 2018) followed by *Pinus spp* (Maitre et al., 2016), *Hakea spp* (Maitre et al., 2016) and *Eucalyptus spp* (Maitre et al., 2016). Among the *Acacias*, *Acacia mearnsii* (black wattle) and *Acacia dealbata* (Silver wattle) are the most aggressive invaders of riparian areas (Richardson and Van Wilgen, 2004; van Wilgen and Wilson, 2018), grassland (Yapi et al., 2018) and forest (Chamier et al., 2012; van Rensburg, 2017) ecosystems in South Africa. As pointed out by Moyo and Fatunbi (2010), there was a streamflow reduction after the infestation of *A. mearnsii* in riparian areas in South Africa. Furthermore Yapi et al. (2018), demonstrated intensifying wildfires and a decrease in agricultural productivity in rangelands and farming areas invaded by *A.*

* Corresponding author at: Discipline of Geography, School of Agricultural, Earth and Environmental Sciences, University of KwaZulu-Natal, Private Bag X01, Scottsville, Pietermaritzburg, 3209, South Africa.
E-mail address: cecilia.mulukwane@gmail.com (C. Masemola).

https://doi.org/10.1016/j.jag.2020.102207
Received 9 April 2020; Received in revised form 17 July 2020; Accepted 20 July 2020
0303-2434/ © 2020 The Authors. Published by Elsevier B.V. This is an open access article under the CC BY-NC-ND license (http://creativecommons.org/licenses/BY-NC-ND/4.0/).

mearnsii in South Africa.

A fundamental step to eradicate *Acacia* species is to prevent its spread. Previous studies have shown that early detection (Ishii and Washitani, 2013) and rapid responses to invasion are critical steps in the eradication of IAPs. An essential element of early detection is to know the geographic information of the species at the landscape level. Inventorying of species within broad landscapes is costly and time-consuming when using field-based observations (Asner and Martin, 2016; Baldeck and Asner, 2014; Rocchini et al., 2018) and therefore not practical for monitoring purposes (Liang, 2013). In recent years, ground surveys are used in conjunction with remote sensing approaches (Müllerová et al., 2013) to map the presence of IAPs on the landscape (Vila and Ibáñez, 2011; Somers and Asner, 2013a).

Practical application of remote sensing techniques requires an understanding of the spectral differences between IAPs and native species (Ollinger, 2011). Previous research has demonstrated that hyperspectral sensors with many contiguous narrow wavelengths are optimal for detecting subtle spectral differences between species (Bradley, 2014; Skowronek et al., 2017; Somers and Asner, 2013b). However, the high dimensionality of hyperspectral data makes calibration complex and computationally expensive. In addition, spaceborne hyperspectral sensors are rare and commercial airborne campaigns to collect hyperspectral data are expensive. Furthermore, field-scale *in situ* hyperspectral data have seldom been up-scaled and explored at the satellite image level. As a result, hyperspectral data lack operational flexibility and preclude large-scale mapping of IAPs. In terms of the limitations of hyperspectral data, low-cost or freely available satellite data are being explored (Gioria et al., 2016; Müllerová et al., 2017; Somodi et al., 2012). New sensors such as Sentinel-2 multispectral imager (MSI) provide improved temporal and additional spectral bands, such as red-edge bands (Drusch et al., 2012), when compared to widely used Landsat satellites series.

The Sentinel-2 MSI optical remote sensors offers unprecedented opportunities to observe the synoptic distribution of the plant species because of its high revisit frequency, larger coverage and high spatial resolution (Drusch et al., 2012). These together with addition bands that are intrinsically linked to traits of vegetation that is control plants spectral signature makes the sensor to have the potential to be used to develop operational methods for IAPs detection and monitoring. However, since the launch of Sentinel-2 MSI, the data is yet to be explored for mapping and monitoring practices of aggressive *Acacia* trees over a large scale.

Despite these advantages of Sentinel-2 compared to multispectral data such as Landsat, spatial resolution (> 10 m) of Sentinel-2 data can still hinder individual tree-level mapping of IAPs in a highly heterogeneous landscape. This makes Sentinel-2 data acquired from a single phenological period of the vegetation often unable to satisfy detection accuracy of the species. Satellite image time series; provide continuous information of the species, and their integration into species discrimination models often leads to increased detection accuracy. Furthermore, highlight the optimal time window to acquire images to map IAPs. Several studies using time series satellite data (Andrew and Ustin, 2006; Wolkovich and Cleland, 2011; Fridley, 2012; Somodi et al., 2012; Gioria et al., 2016; Müllerová et al., 2017) demonstrated a high potential for IAPs discrimination and some also for mapping. In addition, the research related to our study successfully demonstrated time series remote sensing data for discrimination of invasive Australian native Acacia trees from native species in Hawaiian rainforests trees (Somers and Asner, 2012). In Mediterranean Dune Ecosystem (Große-Stoltenberg et al., 2016; Große-Stoltenberg et al., 2018) investigated the species discrimination based remote sensing data acquired during green-up phenophase of vegetation. In these studies, relatively good discrimination of the Australian species was observed. Time series spectral analysis have enabled improvements in species discrimination and highlighted optimal period of the year suitable for detecting the *Acacias* in their respective study areas. In a previous work (Masemola et al., 2019) we have shown strong spectral separability of *A. mearnsii* from its co-occurring native species using crown-level spectroscopic spectral data. The separability was demostrated to be high during the senescence period (March–April). However, these studies were performed using spectroscopic spectral data has well-known disadvantages associated with up scaling to satellite level, hence is not practical for operational purpose at a landscape level. Moreover, study by Masemola et al., 2019 never explored the flowering phase of *Acacia mearnsii*, which occurs during the dry season in August in South Africa (Morais and Freitas, 2015). Therefore, there is a pressing need for time series spectral dynamics of invasive Acacia trees from freely available multispectral Sentinel-2 remote sensing data. This is important when looking toward reaching better outcome and judgement of the potential of the Sentinel-2 sensed data. More so because the Sentinel2 based time series spectral variation between *Acacia* species (i.e. *Acacia mearnsii* and *Acacia dealbata*) and native species is yet to be established.

Therefore, this study investigated whether high temporal Sentinel-2 MSI data can be useful for discriminating *A. mearnsii and Acacia dealbata from native species* in heterogeneous tree canopies landscape. In this study, we focus on two highly invasive species in South Africa, Acacia mearnsii (Black wattle) and Acacia dealbata (Silver wattle). The species invaded large areas in the riparian and terrestrial landscape creating mono-species clusters of KwaZulu Natal, South Africa. The main aim was to investigate a Sentinel-2 time series spectral bands and vegetation indices method for determining which period of the year is most critical for discriminating *Acacia mearnsii* and *Acacia dealbata* from native tree species at landscape level. We further investigated Sentinel-2 features, which are essential for distinguishing *A. mearnsii* and *Acacia dealbata* from native species.

2. Materials and methods

2.1. Study area

The study area is located at the uThukela District Municipality in KwaZulu-Natal Province, South Africa. To be specific, the area is near Van Reenen's Pass (Lat 28.488023° and Lon 29.301116°) on the Great Escarpment of the Drakensberg. Fig. 1 shows the location of the study area relative to South Africa. The current primary use of the land is ranching and agriculture. According to Mucina and Rutherford (2006) the vegetation in the study area include Drakensberg montane forest, low escarpment moist grassland, Eastern Free State sandy grassland, Eastern mist-belt forest, alluvial wetlands and Basotho montane shrubs.

According to Köppen classification the climate is warm and temperate and is categorised as a subtropical highland climate. The area experiences much less rainfall in winter than in summer. The mean annual temperature is 17.1 °C and receives annual mean precipitation of approximately 700 mm. The geology is mainly Beaufort and a bit of Tarkastad and Molteno. The soil is red, yellow, and an association of well drained Ferralsols, Acrisols and Lixisols. The study area is described by uneven topography of between 1000–2000 m above sea level (Fig. 1).

2.2. Invasive alien plants in the study area

The invasive species of interest was *A. mearnsii*. However, during the field survey, *Acacia dealbata* (silver wattle) was found to invade the study area. *Acacia dealbata* the second most aggressive invasive species after *Acacia mearnsii* in South Africa. Besides, *A. mearnsii* is listed among the 100 most aggressive invaders in the world (Global invasive species database, "One Hundred of the World's Worst Invasive Alien Species (ISSG; 2012). Morphologically, *A. mearnsii* and *A. dealbata* are similar. They are both fast-growing evergreen leguminous trees that can grow up to 30 m high. Their leaves are bi-pinnate, but with different colour and texture. For example, *A. mearnsii* has finely hairy dark olive-green leaves, whereas the leaves of *A. dealbata* are blue-green to a silvery grey

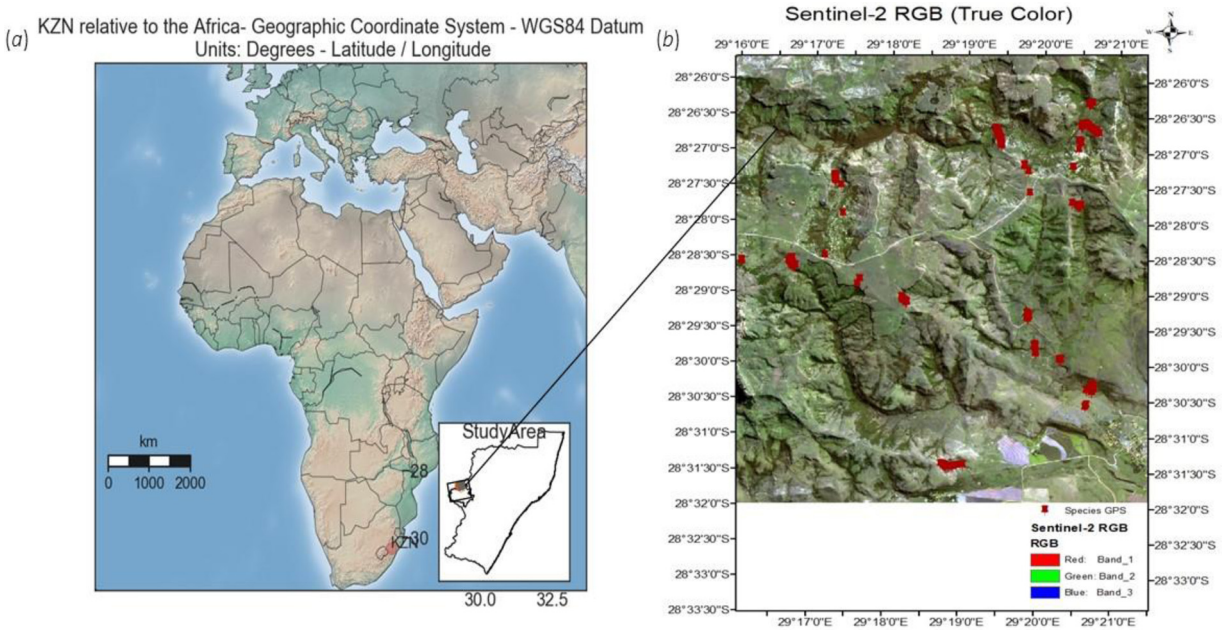

Fig. 1. Location of the study area in KwaZulu Natal, South Africa. (a) Illustrate the location of the study area relative to KwaZulu Natal province, (b) show distribution of species geographic local collected during field survey.

and broad. The greyish silver leaves of *A. dealbata* are the main factor that distinguishes it from *A. mearnsii*. Other than the leaves, the species are more easily distinguished during the flowering season. The flowers of *A. mearnsii* are pale yellow and spherical, whereas *A. dealbata* has bright yellow with globe-shaped heads. In the study area, *A. dealbata* start to bloom from June to August, while the flowers of *A. mearnsii* start to appear in August and peak in September and October (Impson et al., 2008).

2.3. Field data collection

The transect survey was adopted to detect the invasive plants along elevation and soil gradients. We oriented transects in such a way that they start at the lower elevation (next to the river) and end at the high elevation and drier soil. Transects were created by overlaying Sentinel-2 imagery over the study area on Google Earth. About 20 randomly oriented transects of contiguous 30 × 30 m plots that cover Sentinel-2 20m × 20m pixels were created along the transects. The 30 × 30 m plots were created to accommodate 20 × 20 m pixel size of Sentinel-2 imagery. We determined the lengths of the transects based on density and homogeneity of the tree canopies and varied between 50 m and 200 m in length. Longer transects were created for areas with a sparse and high variation of vegetation cover, while shorter ones were for dense and homogeneous cover. Within each plot (30 × 30 m size), we marked and collected geographic coordinates points of each tree species using a handheld Garmin global positioning systems device (accuracy of Garmin). Tree species were identified along transects with the help of a local species expert. Canopies of the species that overlapped one another were sampled separately. Standing dead canopies were not counted but were noted to avoid confusion during classification. Dense patches of *Acacia mearnsii* and *Acacia dealbata* scattered throughout the study area were recorded and polygon were created. Seven hundred and ninety tree canopies were sampled and used for building the training and validation datasets. Based on the species sampled, the area is dominated by *A. mearnsii*, *A. dealbata, Celtis africana, Dais cotinifolia, Diospyros lycioides, Podocarpus latifolius, Searsia Rehmannia, Senegalia caffra, Vachellia sieberiana, Peltophorum africanum* and *Leucosidea sericea* and a summary of the sampled trees is presented in Table 1. In addition, large *Acacia spp* and un-infested (natural forest patches that overlap

Table 1
Summary of different tree species included in discriminating and mapping *Acacia mearnsii* from the study area in the eastern part of Drakensberg great escarpment.

Dominant tree species	Number of canopies per species
Vachellia gerradii	180
Acacia dealbata	150
Acacia mearnsii	166
Podocarpus latifolius	89
Vachellia sieberiana	101
Diospyros lycioides	33
Senelalia caffra	50
Leucosidea sericea	30
Peltophorum africanum	40
Celtis africana	69
Searsia Rehmannia	75

Sentinel-2 pixels were identified in the study area from Google Earth imagery.

2.4. Acquisition and pre-processing of the Sentinel-2 imagery

In total over 12 cloud free images of Sentinel-2 (tile number-L1C_T35JQJ) (Table 2), sensors were obtained from Google Earth

Table 2
Time series Sentinel-2 imagery used in this study.

Months	Sentinel-2 Identification code	Acquisition data
January	L1C_T35JQJ_A013431_20180117T080722	17/01/2018
February	L1C_T35JQJ_A010314_20180226T081205	26/02/2018
March	L1C_T35JQJ_A014432_20180328T081650	28/03/2018
April	L1C_T35JQJ_A005881_20180422T081053	22/04/2018
May	L1C_T35JQJ_A006310_20180522T081541	22/05/2018
June	L1C_T35JQJ_A015719_20180626T081009	26/06/2018
July	L1C_T35JQJ_A016148_20180726T080823	26/07/2018
August	L1C_T35JQJ_A007740_20180830T080723	30/08/2018
September	L1C_T35JQJ_A008026_20180919T081705	19/09/2018
October	L1C_T35JQJ_A017435_20181024T081229	24/10/2018
November	L1C_T35JQJ_A009027_20181128T080926	28/11/2018
December	L1C_T35JQJ_A009127_20181205T080158	05/12/2018

Table 3
Sentinel-2 Multispectral Instrument (MSI) spectral characteristics: band centre and spatial resolution of the ten bands used for the inversion and discrimination of *Acacia mearnsii* from native trees.

Band name	Band width(nm)	Band centre(nm)	Spatial resolution(m)
Blue	96	490	10
Green	45	560	10
Red	39	665	10
Red-edge1	20	704	20
Red-edge2	18	740	20
Red-edge3	28	783	20
Near-Infrared-1	141	842	10
Near-Infrared-2	22	865	20
ShortwaveInfrared-1	142	1610	20
ShortwaveInfrared-2	240	2190	20

Engine's data with 13 spectral bands at 10, 20 and 60 m resolutions. The cloud free georeferenced images were collected between January and December 2018, therefore, covering four South African seasons. Before extracting the Sentinel-2 data, TOA reflectance data were corrected to tree canopy reflectance using iCOR (VITO 2017) available as a plug-in on the Sentinel Application Platform (SNAP) v5.0. According to VITO (2017), iCOR correct Sentinel-2 MSI data by identifying water and land pixels using MODTRAN 5 radiative transfer model Look Up Tables (Berk and Anderson, 2006). More information on the procedure is outlined in VITO (2017). The spectral band's characteristics of Sentinel-2 MSI images are presented in Table 3. The study site is mountainous; as a result, Sentinel Topographic Illumination Correction was performed based on pixel-based Minnaert Correction model (Ge et al., 2008) using 30 m Shuttle Radar Topography Mission (SRTM) Digital Elevation Model downloaded from Google Earth Engine operating system and solar angles from Sentinel-2 scenes metadata.

Image pre-processing, a threshold equal to 0.45 was experimentally selected from the NDVI image in which, grass, bare land, urban land use, water bodies and any other non-crown objects were masked out of the image. Because of this process, resulted images included only areas with the tree canopy.

2.5. Time series spectral information of the species

We extracted Sentinel-2-time series spectral reflectance using species geographical location point at bands shown in Table 2. This was done by overlaying a shape-file format layer created from the the geographic position of the tree species collected during field survey. In addition to spectral bands, we derived vegetation indices from the time series Sentinel-2 images (Table 2) according to the spectral indices package from RStoolbox – CRAN.R-project.org proposed by (Leutner and Horning, 2017) of R statistical software (R Core Team 2018) which was integrated into Python integrated development environment. Subsequently, we stacked all spectral bands and vegetation indices layers and extracted pixel values at species location using the function "rasterstats.*zonal stats*" in the "rasterstats" library (Perry, 2017) in the Python programming language (Sanner, 1999). In total, 98 predictor variables were created from each Sentinel-2 dataset, consisting of spectral bands and vegetation indices related to structural and biochemical properties of the species (Table 4). All extracted predictors were stored in a matrix were columns represented predictors and rows sampled plant species. We used both vegetation indices and reflectance to distinguish IAPs (*A. mearnsii* and *A. dealbata*) from native species using a discriminant random forest (DRF) (Lemmond et al., 2008).

3. Data analysis

3.1. Invasive Acacia species discrimination

To distinguish the IAPs (*A. mearnsii* and *A. dealbata*) from native species in each image, we used the DRF (Lemmond et al., 2008). The DRF is a combination of linear discriminant analysis and conventional Random Forest (RF) classification algorithm (Lemmond et al., 2008). The DRF is an ensemble of decision trees that leverages linear discriminant analysis to perform node splitting and determination of optimal linear decision boundary (Lemmond et al., 2008). Like conventional RF, DRF uses bagging and random feature selection approaches to select essential variables for the classification problem. The model measures variable importance and ranks them using a mean decrease in accuracy, through random permutation. Unlike classical statistical methods, RF does not require a priori assumptions about the nature of the relationships among the response and predictor variables (e.g., remote sensing data) (Breiman, 2001). The algorithm is not affected by distribution (Fu et al., 2012) and redundancy of the data (Fu et al., 2012). Hence, RF produce accurate predictions without overfitting the data regardless of the number of predictors (Breiman, 2001, 2002; Liaw and Wiener, 2002). This also makes RF to be good for spatio-temporal auto correlated data. As a result, RF has been widely used for vegetation classification within the remote-sensing research and applications community (Naidoo et al., 2012; Große-Stoltenberg et al., 2018).

As mentioned before, RF is a decision tree-based classifier. The technique uses the majority vote of the ensemble of trees to identify the species class. The RF require many parameters, but *mtry* (number of variables randomly sampled as candidates at each split) and *ntree* (number of trees to grow) are the most likely to have the biggest effect classification final accuracy (Breiman, 2001). Therefore, only *mtry* and the *ntree* parameters were tuned using grid search parameter tuning strategies in the Scikit-Learn package (Pedregosa et al., 2011) and ten-fold cross validation with five repetitions. The rest of the RF parameters were based on default values. The RF algorithm used recursive feature elimination (RFE) augmented for the internal out-of-bag- error (OOB) (Breiman, 2001) to reduce number of predictors. The classification was implemented using Anaconda (Python 2.8) and the following Packages: GDAL package from OSGEO, OGR, and the Scikit-Learn package (Pedregosa et al., 2011).

3.2. Algorithm performance evaluation metrics

To calibrate and validate the DRF, 780 reflectance and vegetation indices extracted from field sampled tree canopies were randomly separated into calibration (70 % of the points) and the validation (30 % of the points). We first trained the model using 70 % species data. We then used trained model to predict the species based on retained 30 % species dataset. The accuracy of the prediction was assessed using the respective 30 % testing dataset not included in the model training. This was done using MATLAB based multi-class confusion matrix algorithm. Three error statistics (i.e. species-specific accuracy, separability error, sensitivity, specificity, precision, and False Positive Rate, F1-score, Positive Predicted Value (PPV) and Cohen's Kappa) were computed for each species and overall classification of the species. The proposed metrics provided the detailed performance of the classifier and recommended for landscape species mapping by Fielding and Bell (1997) and Lurz et al. (2001). According to Fielding and Bell (1997) & Lurz et al. (2001), sensitivity is conceptually identical to the Producer's Accuracy, while PPV is equivalent to User's Accuracy. In this study, the species mapping models were identified based on sensitivity (Producer's accuracy), PPV, and the Cohen's kappa statistic and the formulas of these metrics are shown in Equations (1)–(4). Producer's accuracy is a metric that measures the probability that the species will be classified an *A. mearnsii* if it is *A. mearnsii*.

$$\%Accuracy = \frac{\text{Obtained result} - \text{expected result}}{\text{expected result}} \times 100 \quad (1)$$

Where percentage Accuracy, is the percentage of correctly classified species class out of all classes.

Table 4
Vegetation Indices Used for Australia native acacias discrimination from native trees in Kwa-Zulu Natal, South Africa. The indices were formulated using Sentinel-2 bands.

Name	Abbrev	Formula	Reference
Anthocyanin reflectance index	ARI	1.0 / B03−1.0 / B05	Gitelson et al. (2009)
Canopy Chlorophyll Content Index	CCCI	((B08 - B05) / (B08 + B05)) / ((B08 - B04) / (B08 + B04))	El-Shikha et al. (2008)
Chlorophyll Green	Chlgreen	([760:800]/[540:560])^(-1)	Gitelson et al. (2006)
Chlorophyll Index Green	CIgreen	B08 / B03−1.0	Ahamed et al. (2011); Gitelson et al. (2003); Hunt et al. (2011);
Chlorophyll Index RedEdge	CIrededge	B08 / B05−1.0	Ahamed et al. (2011); Gitelson et al. (2003); Hunt et al. (2011);
Chlorophyll Red-Edge	Chlred-edge	((B07 / B05), (-1.0))	Gitelson et al. (2006)
Chlorophyll vegetation index	CVI	B08 * B04 / pow(B03, 2.0)	Gobron et al. (2000)
Carotenoid reflectance index 550	CRI550	pow(B02, (-1.0)) - pow(B03, (-1.0))	Gitelson et al. (2001a)
Carotenoid reflectance index 700	CRI700	pow(B02, (-1.0)) - pow(B05, (-1.0))	Merzlyak et al. (2003)
Datt1	Datt1	(B08 - B05) / (B08 - B04)	Datt (1999a); (1999b)
Datt4	Datt4	B04 / (B03 * B05)	Datt (1998)
Datt6	Datt6	B8A / (B03 * B05)	Datt (1998)
Green Difference Vegetation Index	GDVI	B08 - B03	Tucker (1979a)
Enhanced Vegetation Index	EVI	2.5 * (B08 - B04) / ((B08 + 6.0 * B04−7.5 * B02) + 1.0)	Huete et al. (2002)
Enhanced Vegetation Index 2	EVI2	2.4 * (B08 - B04) / (B08 + B04 + 1.0)	Jiang et al. (2008)
Enhanced Vegetation Index 2−2	EVI2.2	2.5 * (B08 - B04) / (B08 + 2.4 * B04 + 1.0)	Jiang et al. (2008)
Green leaf index	GLI	(2.0 * B03 - B04 - B02) / (2.0 * B03 + B04 + B02)	Gobron et al. (2000)
Green Normalized Difference Vegetation Index	GNDVI	(B08 - B03) / (B08 + B03)	Gitelson et al. (1996)
Leaf Chlorophyll Index	LCI	(B08 - B05) / (B08 + B04)	Datt (1999a); (1999b)
Maccioni	Maccioni	(B07 - B05) / (B07 - B04)	(Maccioni et al., 2001)
MCARI/OSAVI	MCARI/OSAVI	((B05 - B04) - 0.2 * (B05 - B03) * (B05 / B04)) / ((1.0 + 0.16) * (B08 - B04) / (B08 + B04 + 0.16))	Wu et al. (2008)
Modified Chlorophyll Absorption in Reflectance Index	MCARI	((B05 - B04) - 0.2 * (B05 - B03)) * (B05 / B04)	Gitelson et al. (2001a), 2001b; Gitelson et al., 2009)
Modified Chlorophyll Absorption in Reflectance Index 1	MCARI1	1.2 * (2.5 * (B08 - B04) - 1.3 * (B08 - B03))	Haboudane et al. (2004)
Modified NDVI	mNDVI	(B08 - B04) / (B08 + B04−2.0 * B01)	Main et al. (2011)
Modified Simple Ratio	mSR	(B08 - B01) / (B04 - B01)	Sims and Gamon (2002)
Normalized Difference 550/450 Plant pigment ratio	PPR	(B03 - B01) / (B03 + B01)	Metternicht (2003)
Normalized Difference 819/1600 NDII	NDII	(B08 - B11) / (B08 + B11)	Henrich et al. (2011); Serrano et al. (2000)
Normalized Difference 819/1649 NDII 2	NDII2	(B08 - B11) / (B08 + B11)	Henrich et al. (2011); Serrano et al. (2000)
Normalized Difference Vegetation Index	NDVI	(B08 - B04) / (B08 + B04)	Tucker (1979b)
Normalized Difference NIR/Rededge Normalized Difference Red-Edge	NDRE	(B08 - B05) / (B08 + B05)	(Barnes et al., 2000a, 2000b)
Optimized Soil Adjusted Vegetation Index	OSAVI	(1.0 + 0.16) * (B08 - B04) / (B08 + B04 + 0.16)	Rondeaux et al. (1996); Haboudane et al. (2002)
Infrared percentage vegetation index	IPVI		Crippen (1990)
Perpendicular Vegetation Index	PVI	(B08 - B04) / sqrt(B08 + B04) * 0.5	
Red edge 1	Rededge1	B05 / B04	Cloutis et al. (1996)
Red edge 2	Rededge2	(B05 - B04) / (B05 + B04)	Cloutis et al. (1996)
Red-edge inflection point1	REIP1		Vogelmann et al. (1993); Clevers et al. (2002); le Maire et al. (2004); Schlerf et al. (2005); Herrmann et al. (2011)
Red-edge inflection point2	REIP2		Vogelmann et al. (1993); Clevers et al. (2002); le Maire et al. (2004); Schlerf et al. (2005); Herrmann et al. (2011)
Red-edge inflection point3	REIP3		Vogelmann et al. (1993); Clevers et al. (2002); le Maire et al. (2004); Schlerf et al., 2005; Herrmann et al. (2011)
Red-Blue NDVI	RBNDVI	(B08 - (B04 + B02)) / (B08 + (B04 + B02))	Wang et al. (2007)
Renormalized Difference Vegetation Index	RDVI	(B08 - B04) / sqrt(B08 + B04) * 0.5	(Broge and Leblanc, 2001)
Soil Adjusted Vegetation Index	SAVI	(B08 - B04) / (B08 + B04 + L) * (1.0 + L (L = 0.428)	(Huete, 1988)
Soil and Atmospherically Resistant Vegetation Index 2	SARVI2	2.5 * (B08 - B04) / (1.0 + B08 + 6.0 * B04−7.5 * B02)	Kaufman and Tanre (1992)
Soil and Atmospherically Resistant Vegetation Index 3	SAVI3	(1.0 + 0.5) * (B08 - B04) / (B08 + B04 + 0.5)	Kaufman and Tanre (1992)
Specific Leaf Area Vegetation Index	SLAVI	B08 / (B04 + B12)	Lymburner et al. (2000)
Structure Intensive Pigment Index 1	SIPI1	(B08 - B01) / (B08 - B04)	Peñuelas et al. (1995)
Structure Intensive Pigment Index 3	SIPI3	(B08 - B02) / (B08 - B04)	Peñuelas et al. (1995)
TCARI/OSAVI	TCARI/OSAVI	(3.0 * (B05 - B04) - 0.2 * (B05 - B03) * B05 / B04) / ((1.0 + 0.16) * (B08 - B04) / (B08 + B04 + 0.16))	Haboudane et al. (2002)
Transformed Chlorophyll Absorption Ratio	TCARI	3.0 * ((B05 - B04) - 0.2 * (B05 - B03) * (B05 / B04))	Daughtry et al. (2000)
Transformed Soil Adjusted Vegetation Index 2	TSAVI	(a * B08 - a * B04 - b) / (B04 + a * B08 - a * b)	Rondeaux et al. (1996)
Transformed Vegetation Index	TVI	sqrt((((B04 - B03) / (B04 + B03))) + 0.5)	Rouse et al. (1974)
Triangular chlorophyll index	TCI	1.2 * (B05 - B03) - 1.5 * (B04 - B03) * sqrt(B05 / B04)	Haboudane et al. (2008); Hunt et al.(2011)
Vegetation Index 700	VI700	(B05 - B04) / (B05 + B04)	Gitelson et al. (2002)
Visible Atmospherically Resistant Index Green	VARI_green	(B03 - B04) / (B03 + B04 - B02)	Gitelson et al. (2002)
Visible Atmospherically Resistant Indices 700	VARI700	(B05−1.7 * B04 + 0.7 * B02) / (B05 + 2.3 * B04−1.3 * B02)	Gitelson et al. (2001b)

(*continued on next page*)

Table 4 (*continued*)

Name	Abbrev	Formula	Reference
Visible Atmospherically Resistant Indices Red Edge	VARI_rededge	(B05 - B04) / (B05 + B04)	Gitelson et al. (2001b)
Weighted Difference Vegetation Index	WDVI	B08 - a * B04 (a = 0.460)	Clevers (1991)
Wide Dynamic Range Vegetation Index	WDRVI	(0.1 * B08 - B04) / (0.1 * B08 + B04)	Gitelson (2004)

$$Sensitivity = \frac{TP}{TP + FN} (\text{Equivalent to Producer's Accuracy}) \quad (2)$$

$$PPV = \frac{TP}{TP + FP} (\text{Equivalent to User's Accuracy}) \quad (3)$$

$$Cohen's kappa = \frac{O - E}{1 - E'} \quad (4)$$

Where:

O and E are observed accuracy and the expected accuracy due to chance, respectively.

3.3. Development of Acacias distribution maps

To produce species distribution maps of *A. mearnsii* and *A. dealbata* among native species, the DRF models with highest accuracy were then applied to the Sentinel-2 images with a pixel size of 20 m. We mapped the species using "RF-predict" function implemented in the GDAL and OSGEO Python libraries. We validated the accuracy of the final species maps by comparing produced maps against the independent sample of species collected during field survey and randomly from Google Earth imagery coinciding with our field survey. The accuracies were evaluated using multiclass error matrix described in Section 3.1.

4. Results

4.1. Time series Sentinel-2 bands discriminatory power for Acacia species from native species using discriminant random forest

Table 5, presents per species and overall species discrimination statistics yielded using DRF model built and validated with Sentinel-2 spectral reflectance. Our results show that *Acacia mearnsii* and *Acacia dealbata* are highly separable from co-occurring native trees with accuracy ranging from 80 % to 92 % (Table 5) which is indicative of high spectral variability with that of co-occurring native species. The overall classification accuracy using spectral reflectance range for 69%–82%. However, the accuracies of *Acacia* species discrimination with DRF were dependent on the period time of image collection and spectral features of the species. The discrimination accuracy assessment result as summarized in Table 5 indicates that an overall accuracies greater than 80 % were obtained for the Sentinel data collected during peak biomass (February), peak flowering (September) and from the start of green to peak productivity seasons (December to January) in southern Africa. The overall discrimination accuracies using DRF was the lowest from image collected in the months April and May (leaf fall) (Table 5). Important feature selection assessment showed that classification executed in these months based on mainly on, red-edge, NIR and SWIR bands, which are highly correlated to biochemical properties of vegetation.

4.2. Performance of time series Sentinel-2 vegetation indices for discrimination between invasive Acacia and native tree species

Table 6 illustrates the performance accuracies of Sentinel-2 derived vegetation indices time-series in distinguishing invasive *Acacia* species from native plants in studied area. The results showed that the vegetation indices were successful in differentiating *Acacia* species from co-occurring native plants. As can be seen in Table 6, over the entire time profile vegetation indices obtained overall accuracies slightly greater than that of spectral reflectance model (range from 76 % to 85 %). The discrimination accuracy assessment result as summarized in Table 6 indicates that an overall accuracies greater than 80 % were obtained for the Sentinel data collected during peak biomass (February-March), Winter (July), peak flowering (September to October) and from the start of green to peak productivity seasons (December to January) in southern Africa. The overall discrimination accuracies using DRF was the lowest from image collected in the month of August (Table 6). Important feature selection assessment showed that classification executed in these months based on mainly on, red-edge, NIR and SWIR bands, which are highly correlated to biochemical properties of vegetation. Vegetation indices that are highly correlated with leaf area index, nitrogen and pigment-based indices produces better discrimination of *Acacias* from native trees than do other species properties-based indices. However, indices that showed high separability between Acacias and natives are those derived with spectral reflectivity in red-edge, NIR and SWR1 wavebands (Fig. 3). Contrary to results obtained by DRF and spectral bands, spectral indices were able to distinguish between *Acacia* species and native species also in April, June, July, September and December with accuracy greater than 80 %. Overall, the accuracy and kappa coefficient ranged from 60 % to 84 % and 0.62 to 0.79, throughout the year.

4.3. Optimal predictors for Acacia spp modeling

Optimal predictors for *Acacia spp* modeling were derived from the variable importance plots depicted in Fig. 2. Fig. 2 show the most important spectral bands and vegetation indices in months that predicted species with high overall accuracy. Fig. 2 show all red-edge, NIR and SWIR to be better predictors of the *Acacia spp.* For Sentinel-2 spectra indices, the most important predictors were mainly biochemical vegetation indices, followed by biophysical related spectral indices (Fig. 2). Similar to spectral bands, the most spectral indices are mainly those calculated with red-edge, NIR and SWIR Sentinel-2 bands. The plots for the combined spectral indices and spectral bands revealed that the vegetation indices are superior, as they are mostly prominent than the spectral bands for all months that yielded high overall accuracy (Fig. 2). In general, vegetation indices have been found to be more suitable for *Acacia spp* mapping than most spectral bands, especially those derived with red-edge, NIR Sentinel-2 bands. Fig. 3 present variable important plots of the annual time series of Sentinel-2, which were analysed to infer optimal periods for image acquisition in *Acacia spp* mapping. Fig. 3, indicate that most important features were from images acquired in the leaf green-up, senescence and flowering (September-October) period of *Acacia* species. Furthermore, Fig. 3 showed that some important variables from images acquired in the dry season (July).Overall Fig. 3 revealed that *Acacia spp* are detectable with Sentinel -2 spectral information in all seasons.

4.4. Spatial distribution of Acacias and native species

Fig. 4 shows the modelled *Acacia* and native species map of the study area. Non-vegetation, water bodies, grass and shrubs were masked out of the results. We produces the species distribution maps using model yielded higher per-species and overall classification accuracies. Statistics relating species distribution maps in Fig. 4 (generated using DRF) with field sampled species information have been

Table 5
Results for the species-specific and overall classification accuracies obtained using the DRF classifier and time-series spectral bands of *Acacias* and combined native species classes.

		Statistic metrics for the performance of the model				
Month	Species	Accuracy	Sensitivity	Specificity	Precision	Kappa
January	Native trees	81.30 %	81.30 %	92.3 %	89.3 %	072
	A. dealbata	81.80 %	81.80 %	92.1 %	83.6 %	075
	A. mearnsii	88.80 %	88.80 %	93.2 %	89.5 %	083
	Overall	82.60 %	82.60 %	85.6 %	90.4	079
February	Native trees	81.9 %	81.90 %	90.2 %	81.4 %	069
	A. dealbata	79.2 %	79.20 %	89.5 %	80.6 %	073
	A. mearnsii	86.6 %	86.6 %	91.3 %	86.5 %	079
	Overall	80.5 %	80.50 %	86.3 %	88.2 %	075
March	Native trees	77.4 %	77.4 %	90.3 %	77.8 %	062
	A. dealbata	70.4 %	70.4 %	91.3 %	75.3 %	066
	A. mearnsii	83.2 %	83.2 %	90.2 %	83.6 %	074
	Overall	75.2 %	75.2 %	88.9 %	78.3 %	069
April	Native trees	69.2 %	69.2 %	88.6 %	69.8 %	069
	A. dealbata	63.6 %	63.6 %	89.1 %	64.5 %	064
	A. mearnsii	91.4 %	91.4 %	90.2 %	91.5 %	081
	Overall	65.9 %	65.9 %	88.3 %	69.5 %	069
May	Native trees	72.2 %	72.2 %	88.6 %	76 %	078
	A. dealbata	64.2 %	64.2 %	86.5 %	86 %	076
	A. mearnsii	85.8 %	85.8 %	90.2 %	85.6 %	073
	Overall	68.6 %	68.6 %	89.2 %	87.3 %	070
June	Native trees	69.2 %	69.2 %	87.3 %	80.9 %	065
	A. dealbata	63.6 %	63.6 %	82.3 %	78.9 %	061
	A. mearnsii	92.9 %	92.9 %	89.6 %	89.3 %	072
	Overall	78.5 %	78.5 %	84.6 %	86.5 %	068
July	Native trees	80.40 %	80.40 %	90.2 %	82.7 %	066
	A. dealbata	72.9 %	72.9 %	91.5 %	90.2 %	069
	A. mearnsii	91.40 %	91.40 %	94.3 %	89.3 %	078
	Overall	76.17 %	76.17 %	88.9 %	84.8 %	072
August	Native trees	70.2 %	70.2 %	90.1 %	80.9 %	066
	A. dealbata	80.5 %	80.5 %	89.8 %	89.2 %	070
	A. mearnsii	84.9 %	84.9 %	86.9 %	89.8 %	075
	Overall	69.6 %	69.6 %	84.9 %	78.9 %	0762
September	Native trees	82.2 %	82.2 %	90.3 %	82.7 %	076
	A. dealbata	73.4 %	73.4 %	98.3 %	79.8 %	078
	A. mearnsii	90.2 %	90.2 %	96.1 %	90.4 %	085
	Overall	81.30 %	81.30 %	86.6 %	80.4 %	073
October	Native trees	78.40 %	78.40 %	91.3 %	89.2 %	075
	A. dealbata	74.5 %	74.5 %	89.6 %	88.6 %	073
	A. mearnsii	89.2 %	89.2 %	90.2 %	89.5 %	083
	Overall	75.2 %	75.2 %	88.4 %	81.5 %	068
November	Native trees	80.60 %	80.60 %	90.3 %	88.6 %	068
	A. dealbata	85.30 %	85.30 %	89.5 %	84.5 %	076
	A. mearnsii	89.6 %	89.6 %	90.6 %	89.6 %	081
	Overall	80.5 %	80.5 %	89.6 %	82.5 %	072
December	Native trees	82.80 %	82.80 %	82.80	78.9	0.75
	A. dealbata	90.60 %	90.60 %	90.60	90.2	0.86
	A. mearnsii	92.80 %	92.80 %	92.80	91.3	0.88
	Overall	82.50 %	82.50 %	82.50	84.3	0.76

reported in Table 6. In most cases, *A. dealbata* was misclassified as native. The separation between invasive and native species is more apparent compared to that between the two invasive species. In general, the result demonstrated a high potential of Sentinel-2 MSI images for the mapping of *A. mearnsii* as well as *A. dealbata* in a mixed species landscape.

5. Discussion

Previous studies have applied similar ideas to detect and map spatial distribution of invasive *Acacia* species. However, most of them have mapped the species using expensive and low temporal resolution remote sensing data such as airborne hyperspectral (Große-Stoltenberg et al., 2018) and LIDAR imagery (Große-Stoltenberg et al., 2018) or an unmanned aerial vehicle (de Sá et al., 2018). However, effective monitoring and management of invasive alien species requires remote sensing data with high revisit frequency and ability to produce continuous distribution maps of species. This study explored the usefulness of multidate Sentinel-2 satellite images in invasive *Acacia* species discrimination and mapping in mountainous infested forest landscape in Kwa-Zulu Natal province, South Africa. This is important because Sentinel -2 MSI has in addition to the traditional visible, NIR and SWIR bands, three additional red-edge bands that allow for the retrievals of concentrations of chlorophyll-a (Chl) or other pigments vegetation analysis. This certainly makes MSI more powerful and worth exploring in identifying areas invaded by invasive *Acacia* species. Both Sentinel-2 spectral reflectance and derived vegetation indices were used as predictors using Discriminant Random Forest Classifier (DRF).The results of this study found Sentinel-2 spectral reflectance and derivatives to be suited for invasive *Acacia* species discrimination and mapping at large scale.

Our Sentinel-2 time series analyses highlighted the optimal time of Sentinel-2 image acquisition for distinguishing and mapping *Acacia dealbata* and *Acacia mearnsii* within co-occurring native plants. In addition, the Sentinel-2 derivatives linked to variations and discrimination and mapping of the species were revealed. Sensitivity and PPV

Table 6
Statistics to compare the accuracy of the Sentinel-2 derived vegetation indices for discriminating invasive *Acacia spp* from native species using discriminant random forest classifier.

		Statistic metrics for the performance of the model				
Month	Species	Accuracy	Sensitivity	Specificity	Precision	Cohen Kappa
January	Native trees	81 %	81 %	91 %	81 %	072
	A. dealbata	82 %	82 %	91 %	83 %	075
	A. mearnsii	89 %	89 %	94 %	89 %	082
	Overall	85 %	85 %	90 %	8432	080
February	Native trees	81 %	81 %	90 %	81 %	069
	A. dealbata	79 %	79 %	90 %	80 %	073
	A. mearnsii	87 %	87 %	93 %	86 %	079
	Overall	83 %	83 %	90 %	82 %	075
March	Native trees	77 %	77 %	88 %	77 %	062
	A. dealbata	70 %	70 %	86 %	70 %	060
	A. mearnsii	82 %	82 %	92 %	83 %	074
	Overall	80 %	80 %	90 %	80 %	070
April	Native trees	69 %	69 %	85 %	69 %	055
	A. dealbata	63 %	63 %	83 %	64 %	051
	A. mearnsii	91 %	91 %	95 %	91 %	080
	Overall	76 %	76 %	90 %	88 %	076
May	Native trees	72 %	72 %	86 %	72 %	057
	A. dealbata	64 %	64 %	83 %	64 %	054
	A. mearnsii	85 %	85 %	92 %	85 %	071
	Overall	73 %	73 %	90 %	82 %	063
June	Native trees	69 %	69 %	85 %	69 %	055
	A. dealbata	63 %	63 %	83 %	64 %	051
	A. mearnsii	91 %	91 %	95 %	91 %	080
	Overall	76 %	76 %	90 %	88 %	073
July	Native trees	79 %	79 %	90 %	80 %	066
	A. dealbata	73 %	73 %	87 %	73 %	069
	A. mearnsii	91 %	91 %	96 %	91 %	082
	Overall	80 %	80 %	92 %	88 %	074
August	Native trees	82 %	82 %	91 %	82 %	069
	A. dealbata	73 %	73 %	88 %	73 %	070
	A. mearnsii	90 %	90 %	95 %	90 %	080
	Overall	79 %	79 %	90 %	88 %	076
September	Native trees	78 %	78 %	89 %	78 %	066
	A. dealbata	74 %	74 %	88 %	74 %	070
	A. mearnsii	89 %	89 %	94 %	89 %	077
	Overall	85 %	80 %	89 %	86 %	073
October	Native trees	80 %	80 %	91 %	81 %	073
	A. dealbata	85 %	85 %	92 %	84 %	079
	A. mearnsii	89 %	89 %	94 %	89 %	081
	Overall	83 %	83 %	90 %	88 %	078
Nov	Native trees	82 %	82 %	91 %	82 %	076
	A. dealbata	90 %	90 %	95 %	91 %	085
	A. mearnsii	93 %	93 %	96 %	91 %	084
	Overall	86 %	85 %	93 %	89 %	080
Nov	Native trees	83 %	83 %	89 %	85 %	073
	A. dealbata	92 %	92 %	92 %	93 %	080
	A. mearnsii	90 %	90 %	90 %	90 %	081
	Overall	83 %	80 %	90 %	88 %	076

values for spectral reflectance and spectral indices based classification models were found to be higher between invasive Acacias and native species and for overall classification in most of the sentinel-2 images. These results with the Random Forest algorithm are consistent with previous studies in the field of Remote Sensing of Australia native *Acacia* species (Große-Stoltenberg et al., 2018).

Sentinel-2 multitemporal spectra of targeted area shows a clear distinction between *Acacia* spp and native species, in the beginning of the growing season (November–January) (Cho et al., 2017) and peak vegetation productivity (February-mid March) (Cho et al., 2017) in South Africa. This can be attributed to the trait dissimilarity in leaf biochemistry between invasive *Acacia spp*. and native species reported in previous studies (Große-Stoltenberg et al., 2018; Masemola et al., 2019). Contrary to expectations, spectra reflectance extracted from Sentinel-2 image acquired in April (senescence for deciduous plants) failed to improve discrimination between invasive Acacia. spp native species. This was unexpected because evergreen plants (e.g. A. dealbata and A. mearnsii) are known to show different spectral signature to that of deciduous vegetation (native species) during senescence period in southern Africa (Cho et al., 2012; Madonsela et al., 2017). According to Cho et al. (2017), there is a strong spectral distinction between deciduous and evergreen tree canopies during senescence vegetation phase because of biochemical contents variation, mainly chlorophyll, nitrogen and water. We also observed spectral differences during dry season (18 July 2018) and then significantly decreases at the beginning of flowering season (August) for *Acacia spp*. Although the results indicated that multi-date spectral reflectance effectively discriminated and revealed optimal dates for mapping *Acacia spp*, more optimal dates were revealed by spectral indices based modelling.

Sentinel-2 data vegetation indices based model achieved the more optimal and high accuracy when compared to spectral reflectance model. For example, in vegetation indices analysis revealed discrimination between Acacia spp and native spp during transition from peak productivity to senescence of deciduous vegetation (i.e. April), Winter (June –July), peak flowering period of *Acacias* (September) and early summer (December). In the studied area, in winter (leaf-off

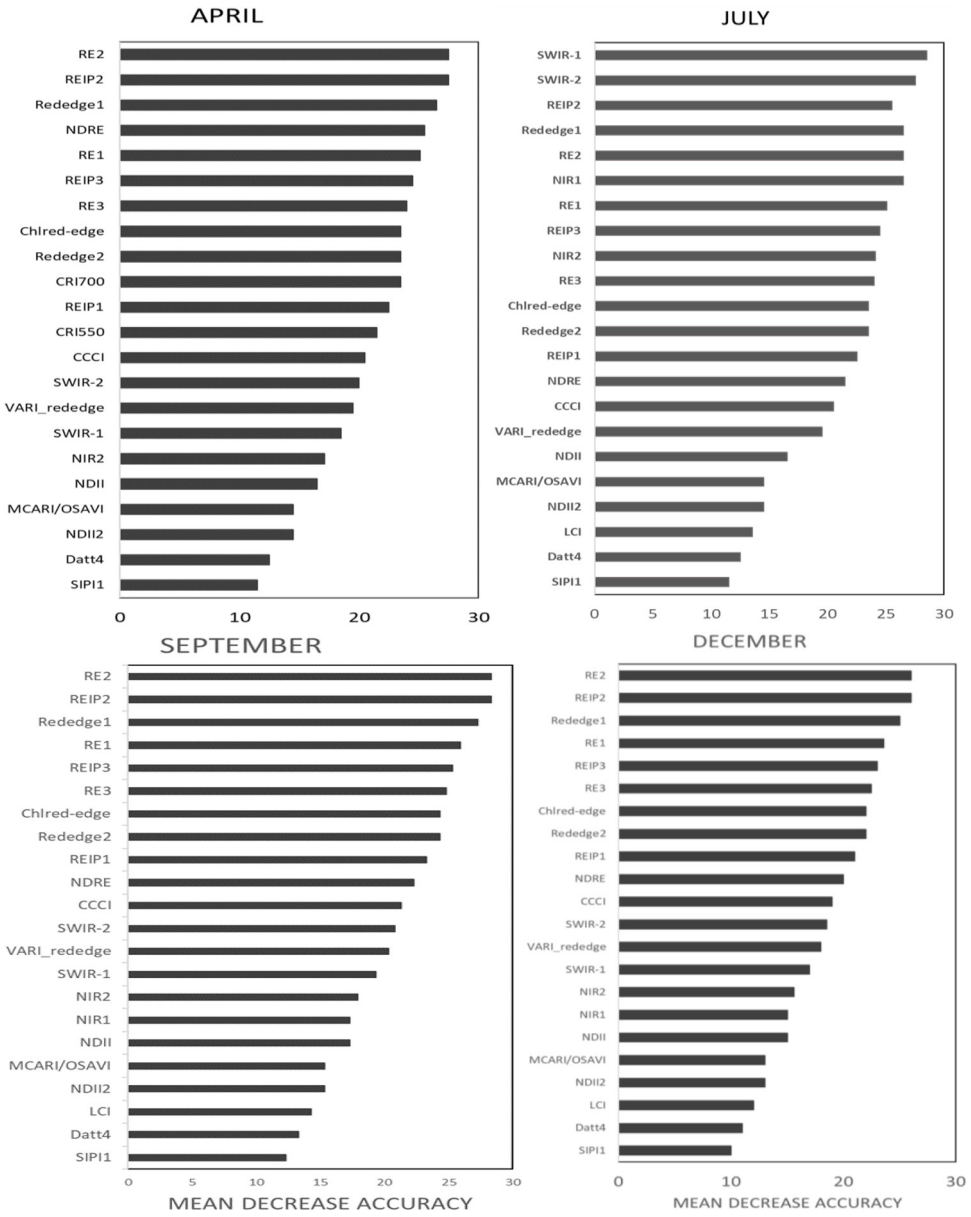

Fig. 2. Twenty-five most important variables (spectral indices and spectral bands for *Acacia* species discrimination regrading selected important months according to Mean Decrease Accuracy.

period) branches of deciduous vegetation are exposed (Laurin et al., 2018) due to their desiccation phase and lack of nutrients. Previous remote sensing-based studies conducted in South Africa also indicated that senescence and winter seasons are crucial for the discrimination of deciduous and evergreen vegetation (Cho et al., 2012; Madonsela et al., 2017). Previous research has found invasive Acacia spp and non-Acacia native species to show differences in terms of biochemical traits (Große-Stoltenberg et al., 2018). Thus, we attribute the high predictive performances of spectral indices to their capabilities to maximize sensitivity to vegetation traits. At heterogeneous landscape of tropical rainforest trees, Clark and Roberts (2012) using spectrometer remote sensing data also discriminated one of the Australia native *Acacias* (i.e. *Acacia Longifolia*) based on spectral derivatives sensitive to biochemical characteristics of vegetation. This also complies with Große-Stoltenberg et al. (2018) study that found spectral distinction between Australia native Acacias and non-acacias based on spectral properties linked to LAI, chlorophyll and nitrogen content. This finding confirms the suggestion by Asner and Martin (2016), that species biochemistry and biophysical properties can facilitate the mapping of invasive species distribution.

Important feature identification analysis in this study provides new information on the use of Sentinel- 2 optimal predictors for Acacia spp prediction and mapping in the studied area. The results showed that the Sentinel-2 red-edge spectral bands and associate indices proved to be superior to the commonly used red and near–infrared canopy reflectance and indices for *Acacia spp* prediction and mapping. Results suggested that these features could accurately predict invasive *Acacia spp* and yield consistent predictive performances across temporal scales. The CIrededge, Chlred-edge, MCARI/OSAVI,VARIrededge, NDRE, REIP1, REIP2, REIP3, mNDVI, NDII2, EVI2.2, LCI, and CCCI, were the most important spectral indices in the prediction of the *Acacia spp* for all images. Other studies that discriminated invasive *Acacia spp* reported the importance of red–edge bands similar results (Große-Stoltenberg et al., 2018). Große-Stoltenberg et al. (2018), for example, using hyperspectral vegetation indices obtained better prediction accuracy with features linked to chlorophyll, carotenoids, and LAI and the red-edge region of the spectrum. According to Laurin et al. (2018) and Mutanga and Skidmore (2004) red-edge derived vegetation

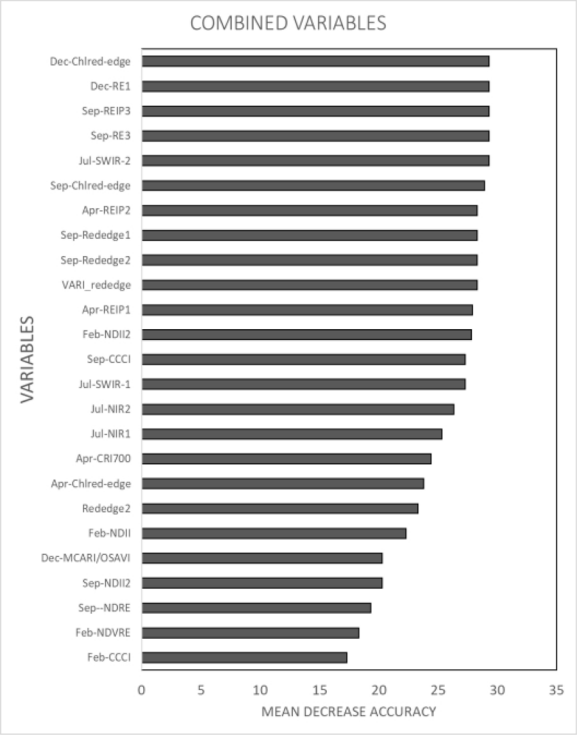

Fig. 3. Top twenty-five most important variables for *Acacia spp* mapping according to Mean Decrease Accuracy and Mean Decrease Gini statistics.

indices mitigate the saturation problem due to large LAI, hence tends to be effective for tree species discrimination. The red-edge spectral information are known to be sensitive to biochemical, particularly leaf chlorophyll that is also highly correlated to leaf nitrogen content. Therefore the performance of red-edge features can be attributed to high nitrogen differences between *Acacia spp* and non-acacia native species reported in Große-Stoltenberg et al. (2018) study. Furthermore, a possible reason for this could be from the fact that Australian *Acacias* are nitrogen fixers (Somers and Asner, 2012; Große-Stoltenberg et al., 2016; Große-Stoltenberg et al., 2018), which makes them to be sensitive to chlorophyll spectral features of the Sentinel-2 data. This suggest that Sentinel -2 features should be considered for improved large scape *Acacia. spp* mapping. Further, the high accuracy of spectral indices from Sentinel-2 data acquired during dry seasons and flowering season of *Acacia spp* can reduce the limitation of cloud interference for optical data and allow accurate mapping of these species. Overall performance of the spectral indices can be attributed to the fact that, they are more capable of reducing variation within canopy species and capture structural and biochemical differences between species, thus improving invasive *Acacia. spp* identification.

Although clear flowering distribution patterns of Acacias were not visible in Sentinel-2 images of studied area, we have proved that the Sentinel-2 spectral information extracted during flowering period of Australian Acacia trees can classify and help to map their distribution at large scale. Similar to our study, Paz-Kagan et al. (2019) identified and mapped the aggressive *Acacia spp* based on their flowering traits with multispectral images data in the coastal plain of Israel. Like in other period of the year, their spectral reflectivity were highly distinctive from that of native species with red-edge Sentinel-2 bands during flowering phase. According to Ge et al. (2006), high variation between the species during peak flowering pheno-phase is mainly characterised by an increased concentration in canopy pigments, nutrients, water contents properties during reproduction period. Their study documented some enhanced spectral dissimilarities between invasive yellow starthistle (Ge et al., 2008) and surrounding native species during peak flowering compared to the start of flowering. Therefore, the highest sensitivity during peak flowering phase (September and November), may be attributed to the enhanced biochemical concentration of *Acacia spp*.

The variable importance plots of all annual spectral reflectance and indices data revealed that images acquired in the wet season (December to March) are important for invasive *Acacia. spp* modelling in the study area. The *Acacia spp* differed greatly with native species over the growing season, dry season and flowering of the *Acacia spp* and the largest distinction occurred during the growing season (November–January) and peak vegetation productivity (February) with spectral indices. Seasonally, *Acacia spp* are more detectable with the spectral indices during dry season than with spectral reflectance. However, the combined use of spectral indices and reflectance data significantly increased species discrimination in most months of the year. In addition, red-edge bands, we found that during wet season NIR and SWIR bands are also important which could be linked to the distinct canopy structure and nitrogen content of *Acacia spp* compared to native species in the study area. This finding is highly important for Acacia spp mapping in southern Africa where optical sensors fail to deliver useful images during the wet season due to excessive cloud cover. This will also allow the use of Landsat data for periods when Sentinel-2 data are not available. In general, this study has shown that dry season images may be sufficient for accurate *Acacia spp* in the grassland regions of South Africa.

The species distribution maps produced in this study are consistent with our field knowledge; A. dealbata dominates along the river while *A. mearnsii* dominates on top of the hill. These findings add to a growing body of literature on remote sensing of invasive Australia native *Acacia spp*. Because of the abundant temporal and spatial information offered by Sentinel -2 data can plays a very significant role for monitoring the spread of *Acacia* species over a large area. It is important and critical that future interdisciplinary research among ecologists should focus on developing an operational system of mapping and monitoring the spatial spread of invasive species using Sentinel-2 data across all types of ecosystems. The maps produced in this study represent unique information for *Acacia spp* monitoring and identification. This can help scientists, land managers and policy makers understand the contribution of invasive *Acacia spp* in various environmental issues. It is also hoped that the study will stimulate the use of remote sensing data for continuous monitoring of the species at national to regional level in Africa.

6. Conclusion

This study demonstrated the efficiency of Sentinel-2 time series features for aggressive Australian Acacias classi- fication at heterogeneous forest landscape. Our study has shown that Sentinel-2 remote sensing data to identify Australian Acacias IPS can be applied at the landscape scale. The analysis demonstrated that additional Sentinel-2 red-edge spectral together with NIR and SWIR bands are significant to modelling and mapping Acacia mearnsii and Acacia dealbata distribution from space. Both Acacia mearnsii and Acacia dealbata could be identified based on canopy spectral information related to LAI, nitrogen and chlorophyll of the species. This were validated by features, which according to the DRF classifier contributed to the high accuracy of the species discrimination. Aggressive invasive Acacia species can be characterised and mapped on a large scale, utilizing their flowering spectral reflectivity. Numerous time window exist that can be used to map both *Acacia mearnsii* and *Acacia dealbata* at landscape level scale. The start of greening, peak productivity, winter and the peak flowerings phase of invasive species were found to yield high pixel-level discrimination of *Acacias* from surrounding native species using Sentinel-2 MSI in natural landscapes. In general, the use of Sentinel-2 time series spectral bands and vegetation indices has increased our understanding of Australian Acacias spectral dynamics, and proved that the sensor is a

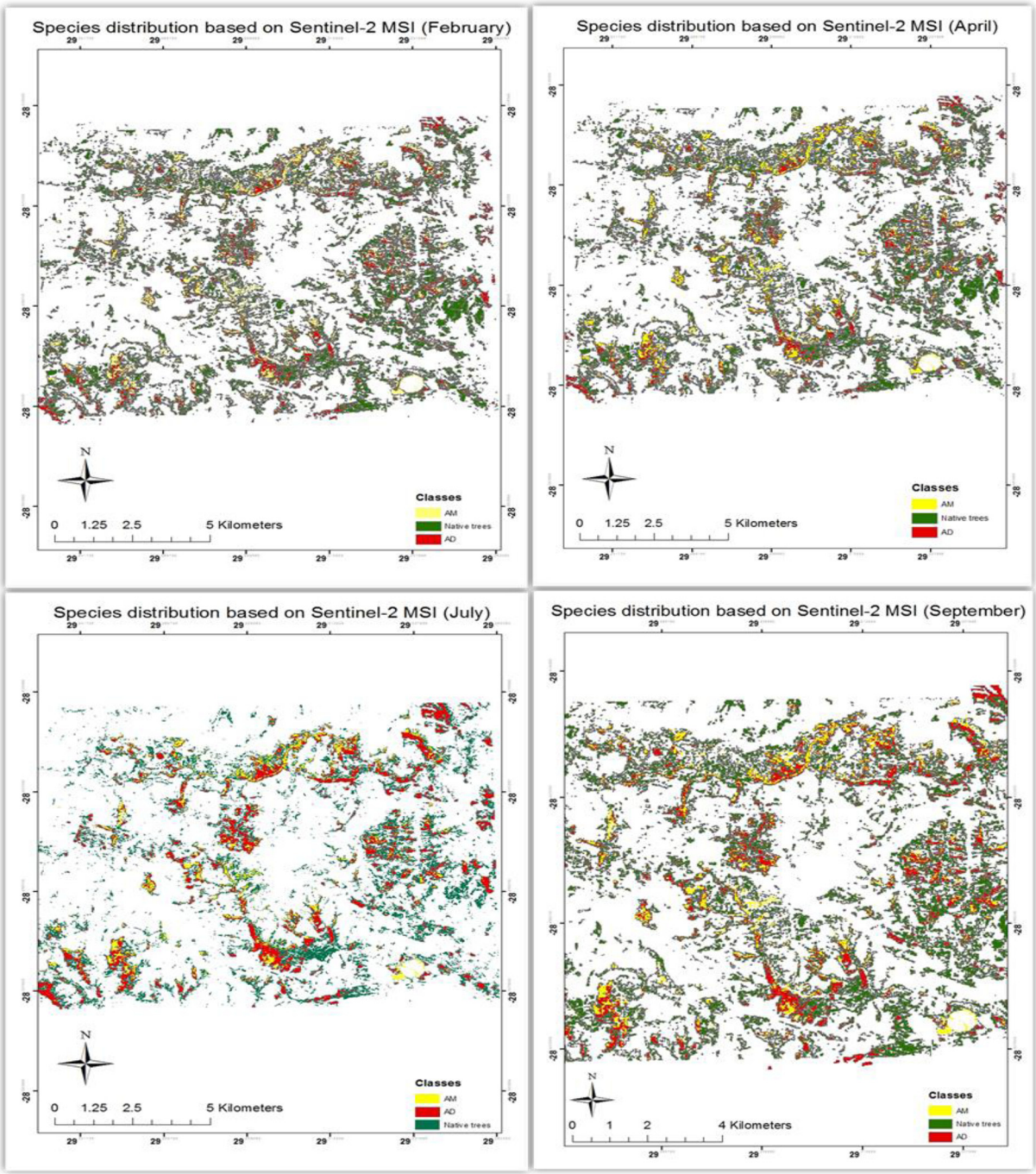

Fig. 4. Invasive tree species distribution in the study area for the best-accuracy classification performed for Sentinel-2 data time series for five imageries. The maps are based on images capture in February, April, July and September. AM = *Acacia mearnsii,* AD = *Acacia dealbata* and native trees = non-invasive native tree species.

useful tool for characterization and monitoring *Acacias* over a large scale. Our results and approach could assist in detailed geographic information of the species and used to assess the spread and severity of invasion. This can enable land managers assess the environmental consequences of *Acacias* as well as to deploy controls on their spread in the South African landscape.

CRediT authorship contribution statement

Cecilia Masemola: Conceptualization, Methodology, Software, Data curation, Writing - original draft, Visualization, Investigation. **Moses Azong Cho:** Supervision, Conceptualization, Writing - review & editing. **Abel Ramoelo:** Supervision, Writing - review & editing.

Declaration of Competing Interest

In accordance with the Journal and my ethical obligation as a researcher, I am reporting that there is no potential conflict of interest to be reported by the authors."

Acknowledgement

The authors would like to thank the Council for Scientific and Industrial Research for providing logistical and funding support for this project.

Appendix A. Supplementary data

Supplementary material related to this article can be found, in the online version, at doi:https://doi.org/10.1016/j.jag.2020.102207.

References

Ahamed, T., Tian, L., Zhang, Y., Ting, K.C., 2011. A Review of Remote Sensing Methods for Biomass Feedstock Production.

Andrew, M.E., Ustin, S.L., 2006. Spectral and physiological uniqueness of perennial pepperweed (Lepidium latifolium). Weed Sci. 54, 1051–1062.

Asner, G.P., Martin, R.E., 2016. Spectranomics: emerging science and conservation opportunities at the interface of biodiversity and remote sensing. Glob. Ecol. Conserv. 8, 212–219.

Baldeck, C.A., Asner, G.P., 2014. Improving remote species identification through efficient training data collection. Remote Sens. (Basel) 6, 2682–2698.

Barnes, E.M., Clarke, T.R., Richards, S.E., Colaizzi, P.D., Haberland, J., Kostrzewski, M., Waller, P., Choi, C., Riley, E., Thompson, T., 2000a. Coincident detection of crop water stress, nitrogen status and canopy density using ground based multispectral data. In: Proceedings of the Fifth International Conference on Precision Agriculture. Bloomington, MN, USA.

Barnes, E.M., Clarke, T.R., Richards, S.E., Colaizzi, P.D., Haberl, J., Kostrzewski, M., et al., 2000b. Coincident detection of crop water stress, nitrogen status and canopy density using ground based multispectral dataed. In: the Fifth International Conference on Precision Agriculture and Other Resource Management. Madison, WI: ASA-CSSA-SSSA.

Berk, A., Anderson, G., … P.A.-A. and, 2006, undefined, n.d. MODTRAN5: 2006 update. spiedigitallibrary.org.

Bradley, B.A., 2014. Remote detection of invasive plants: a review of spectral, textural and phenological approaches. Biol. Invasions 16, 1411–1425.

Breiman, L., 2001. Random forests. Mach. Learn. 45, 5–32. https://doi.org/10.1023/A:1010933404324.

Broge, N.H., Leblanc, E., 2001. Comparing prediction power and stability of broadband and hyperspectral vegetation indices for estimation of green leaf area index and canopy chlorophyll density. Remote Sens. Environ. 76, 156–172.

Cardinale, B.J., Duffy, J.E., Gonzalez, A., Hooper, D.U., Perrings, C., Venail, P., Narwani, A., Mace, G.M., Tilman, D., Wardle, D.A., 2012. Biodiversity loss and its impact on humanity. Nature 486, 59.

Chamier, J., Schachtschneider, K., Maitre, D.C.Le, Ashton, P.J., Van Wilgen, B.W., 2012. Impacts of invasive alien plants on water quality, with particular emphasis on South Africa. Water Sa 38, 345–356.

Cho, M.A., Mathieu, R., Asner, G.P., Naidoo, L., van Aardt, J., Ramoelo, A., Debba, P., Wessels, K., Main, R., Smit, I.P.J., Erasmus, B., 2012. Mapping tree species composition in South African savannas using an integrated airborne spectral and LiDAR system. Remote Sens. Environ. 125, 214–226. https://doi.org/10.1016/j.rse.2012.07.010.

Cho, M.A., Ramoelo, A., Dziba, L., 2017. Response of land surface phenology to variation in tree cover during green-up and senescence periods in the semi-arid savanna of Southern Africa. Remote Sens. 9, 689.

Clark, M.L., Roberts, D.A., 2012. Species-level differences in hyperspectral metrics among tropical rainforest trees as determined by a tree-based classifier. Remote Sens. 4, 1820–1855.

Clevers, J.G.P.W., 1991. Application of the WDVI in estimating LAI at the generative stage of barley. ISPRS J. Photogramm. Remote Sens. 46 (1), 37–47.

Clevers, J., De Jong, S.M., Epema, G.F., Van Der Meer, F.D., Bakker, W.H., Skidmore, A.K., Scholte, K.H., 2002. Derivation of the red edge index using the MERIS standard band setting. Int. J. Remote Sens. 23, 3169–3184.

Cloutis, E.A., Connery, D.R., Major, D.J., Dover, F.J., 1996. Airborne Multi-spectral Monitoring of Agricultural Crop Status: Effect of Time of Year, Crop Type and Crop Condition Parameter.

Crippen, R.E., 1990. Calculating the vegetation index faster. Remote Sens. Environ. 34, 71–73.

Datt, B., 1998. Remote sensing of chlorophyll a, chlorophyll b, chlorophyll a + b, and total carotenoid content in eucalyptus leaves. Remote Sens. Environ. 66, 111–121.

Datt, B., 1999a. A new reflectance index for remote sensing of chlorophyll content in higher plants: tests using Eucalyptus leaves. J. Plant Physiol. 154, 30–36.

Datt, B., 1999b. Remote sensing of water content in Eucalyptus leaves. Aust. J. Bot. 47, 909–923.

Daughtry, C.S.T., Walthall, C.L., Kim, M.S., De Colstoun, E.B., Mcmurtrey, J.E., 2000. Estimating corn leaf chlorophyll concentration from leaf and canopy reflectance. Remote Sens. Environ. 74, 229–239.

de Sá, N.C., Castro, P., Carvalho, S., Marchante, E., López-Núñez, F.A., Marchante, H., 2018. Mapping the flowering of an invasive plant using unmanned aerial vehicles: is there potential for biocontrol monitoring? Front. Plant Sci. 9, 293.

Drusch, M., Del Bello, U., Carlier, S., Colin, O., Fernandez, V., Gascon, F., Hoersch, B., Isola, C., Laberinti, P., Martimort, P., Meygret, A., Spoto, F., Sy, O., Marchese, F., Bargellini, P., 2012. Sentinel-2: ESA's optical high-resolution mission for GMES operational services. Remote Sens. Environ. 120, 25–36. https://doi.org/10.1016/j.rse.2011.11.026.

El-Shikha, D.M., Barnes, E.M., Clarke, T.R., Hunsaker, D.J., Haberland, J.A., Pinter, P.J., et al., 2008. Remote sensing of cotton nitrogen status using the Canopy chlorophyll content index (CCCI). Trans. Asabe 51, 73–82.

Fielding, A.H., Bell, J.F., 1997. A review of methods for the assessment of prediction errors in conservation presence/absence models. Environ. Conserv. 24, 38–49.

Fridley, J.D., 2012. Extended leaf phenology and the autumn niche in deciduous forest invasions. Nature 485, 359.

Fu, H., Zhang, Q., Qiu, G., 2012. Random Forest for Image Annotation, in: Lecture Notes in Computer Science (Including Subseries Lecture Notes in Artificial Intelligence and Lecture Notes in Bioinformatics). pp. 86–99. https://doi.org/10.1007/978-3-642-33783-3_7.

Ge, H., Lu, D., He, S., Xu, A., Zhou, G., Du, H., 2008. Pixel-based minnaert correction method for reducing topographic effects on a landsat 7 ETM+ image. Photogramm. Eng. Remote Sensing 74 (11), 1343–1350. https://doi.org/10.14358/PERS.74.11.1343.

Gioria, M., Pyšek, P., Osborne, B.A., 2016. Timing is everything: does early and late germination favor invasions by herbaceous alien plants? J. Plant Ecol. 11, 4–16.

Gitelson, A.A., 2004. Wide dynamic range vegetation index for remote quantification of biophysical characteristics of vegetation. J. Plant Physiol. 161, 165–173.

Gitelson, A.A., Kaufman, Y.J., Merzlyak, M.N., 1996. Use of a green channel in remote sensing of global vegetation from EOS-MODIS. Remote Sens. Environ. 58, 289–298.

Gitelson, A.A., Merzlyak, M.N., Chivkunova, O.B., 2001a. Optical properties and nondestructive estimation of anthocyanin content in plant leaves. Photochem. Photobiol. 74, 38–45.

Gitelson, A.A., Merzlyak, M.N., Zur, Y., Stark, R., Gritz, U., 2001b. Non-destructive and remote sensing techniques for estimation of vegetation statused. In: Third European Conference on Precision Agriculture. Montpellier, France. pp. 301–306.

Gitelson, A.A., Kaufman, Y.J., Stark, R., Rundquist, D., 2002. Novel algorithms for remote estimation of vegetation fraction. Remote Sens. Environ. 80, 76–87.

Gitelson, Anatoly A., Viña, Andrés, Arkebauer, Timothy J., Rundquist, Donald C., Keydan, Galina, Leavitt, Bryan, 2003. Remote Estimation of Leaf Area Index and Green Leaf Biomass in Maize Canopies.

Gitelson, Anatoly A., Keydan, Galina P., Merzlyak, Mark N., 2006. Three-band Model for Noninvasive Estimation of Chlorophyll, Carotenoids, and Anthocyanin Contents in Higher Plant Leaves.

Gitelson, A.A., Chivkunova, O.B., Merzlyak, M.N., 2009. Nondestructive estimation of anthocyanins and chlorophylls in anthocyanic leaves. Am. J. Bot. 96, 1861–1868.

Gobron, N., Pinty, B., Verstraete, M.M., Widlowski, J.L., 2000. Advanced vegetation indices optimized for up-coming sensors: design, performance, and applications. IEEE Trans. Geosci. Remote. Sens. 38, 2489–2505.

Große-Stoltenberg, A., Hellmann, C., Werner, C., Oldeland, J., Thiele, J., 2016. Evaluation of continuous VNIR-SWIR spectra versus narrowband hyperspectral indices to discriminate the invasive Acacia longifolia within a Mediterranean dune ecosystem. Remote Sens. (Basel) 8, 334.

Große-Stoltenberg, A., Hellmann, C., Thiele, J., Oldeland, J., Werner, C., 2018. Invasive acacias differ from native dune species in the hyperspectral/biochemical trait space. J. Veg. Sci. 29, 325–335.

Haboudane, D., Miller, J.R., Tremblay, N., Zarco-Tejada, P.J., Dextraze, L., 2002. Integrated narrowband vegetation indices for prediction of crop chlorophyll content for application to precision agriculture. Remote Sens. Environ. 81, 416–426.

Haboudane, D., Miller, J.R., Pattey, E., Zarco-Tejada, P.J., Strachan, I.B., 2004. Hyperspectral vegetation indices and novel algorithms for predicting green LAI of crop canopies: modeling and validation in the context of precision agriculture. Remote Sens. Environ. 90, 337–352.

Haboudane, D., Tremblay, N., Miller, J.R., Vigneault, P., 2008. Remote estimation of crop chlorophyll content using spectral indices derived from hyperspectral data. IEEE Trans. Geosci. Remote. Sens. 46, 423–437.

Henrich, V., Krauss, G., Götze, C., Sandow, C., 2011. The IndexDatabase.

Herrmann, I., Pimstein, A., Karnieli, A., Cohen, Y., Alchanatis, V., Bonfil, D.J., 2011. LAI Assessment of Wheat and Potato Crops by VENμS and Sentinel-2 Bands.

Huete, A.R., 1988. A soil-adjusted vegetation index (SAVI). Remote Sens. Environ. 25, 295–309.

Huete, A., Didan, K., Miura, T., Rodriguez, E.P., Gao, X., Ferreira, L.G., 2002. Overview of the radiometric and biophysical performance of the MODIS vegetation indices. Remote Sens. Environ. 83, 195–213.

Hunt Jr., E., Raymond; Daughtry, C.S.T., Eitel, Jan U.H., Long, D.S., 2011. Remote Sensing Leaf Chlorophyll Content Using a Visible Band Index.

Impson, F.A.C., Kleinjan, C.A., Hoffmann, J.H., Post, J.A., 2008. *Dasineura rubiformis* (Diptera: Cecidomyiidae), a new biological control agent for Acacia mearnsii in South Africa. South Afr. J. Sci. 104, 247–249.

Ishii, J., Washitani, I., 2013. Early detection of the invasive alien plant Solidago altissima in moist tall grassland using hyperspectral imagery. Int. J. Remote Sens. 34, 5926–5936.

Jiang, Z., Huete, A.R., Didan, K., Miura, T., 2008. Development of a two-band enhanced vegetation index without a blue band. Remote Sens. Environ. 112, 3833–3845. https://doi.org/10.1016/j.rse.2008.06.006.

Kaufman, Y.J., Tanre, D., 1992. Atmospherically resistant vegetation index (ARVI) for EOS-MODIS. IEEE Trans. Geosci. Remote. Sens. 30, 261–270.

Laurin, G.V., Laurin, G.V., Balling, J., Corona, P., Mattioli, W., Papale, D., Puletti, N., 2018. Above-ground Biomass Prediction by Sentinel-1 Multitemporal Data in Central Italy With Integration of ALOS2 and Sentinel-2 Data. pp. 12. https://doi.org/10.1117/1. JRS.12.

le Maire, G., Francois, C., Dufrene, E., 2004. Towards Universal Broad Leaf Chlorophyll Indices Using PROSPECT Simulated Database and Hyperspectral Reflectance Measurements.

Lemmond, T.D., Hatch, A.O., Chen, B.Y., Knapp, D., Hiller, L., Mugge, M., Hanley, W.G., 2008. Discriminant Random Forests. DMIN, pp. 55–61.

Leutner, B., Horning, N., n.d. RStoolbox: Tools for Remote Sensing Data Analysis. 2017. CRAN–Package RStoolbox.Available online: https://cran.r-project.org/web/packages/RStoolbox/index.html (accessed on 5 February 2018).

Liang, J.R.S., 2013. Remote Sensing of Weed Canopies. From Laboratory Spectroscopy to

Remotely Sensed Spectra of Terrestrial Ecosystems, pp. 175.
Lurz, P.W.W., Rushton, S.P., Wauters, L.A., Bertolino, S., Currado, I., Mazzoglio, P., Shirley, M.D.F., 2001. Predicting grey squirrel expansion in North Italy: a spatially explicit modelling approach. Landsc. Ecol. 16, 407–420.
Lymburner, L., Beggs, P.J., Jacobson, C.R., 2000. Estimation of canopy-average surface-specific leaf area using Landsat TM data. Photogramm. Eng. Remote Sens. 66, 183–191.
Maccioni, A., Agati, G., Mazzinghi, P., 2001. New vegetation indices for remote measurement of chlorophylls based on leaf directional reflectance spectra. J. Photochem. Photobiol. B, Biol. 61, 52–61.
Madonsela, S., Cho, M.A., Mathieu, R., Mutanga, O., Ramoelo, A., Kaszta, Ż., Van De Kerchove, R., Wolff, E., 2017. Multi-phenology WorldView-2 imagery improves remote sensing of savannah tree species. Int. J. Appl. Earth Obs. Geoinf. 58, 65–73.
Main, R., Cho, M.A., Mathieu, R., O'kennedy, M.M., Ramoelo, A., Koch, S., 2011. An investigation into robust spectral indices for leaf chlorophyll estimation. ISPRS J. Photogramm. Remote. Sens. 66, 751–761.
Maitre, D.C. Le, Gaertner, M., Marchante, E., Ens, E., Holmes, P.M., Pauchard, A., O'Farrell, P.J., Rogers, A.M., Blanchard, R., Blignaut, J., 2011. Impacts of invasive Australian acacias: implications for management and restoration. Divers. Distrib. 17, 1015–1029.
Maitre, D.C. Le, Forsyth, G.G., Dzikiti, S., Gush, M.B., 2016. Estimates of the impacts of invasive alien plants on water flows in South Africa. Water SA 42 (4), 659–672.
Marchante, H., Marchante, E., Freitas, H., Hoffmann, J.H., 2015. Temporal changes in the impacts on plant communities of an invasive alien tree, Acacia longifolia. Plant Ecol. 216, 1481–1498.
Masemola, C., Cho, M.A., Ramoelo, A., 2019. Assessing the effect of seasonality on leaf and canopy spectra for the discrimination of an alien tree species, Acacia mearnsii, from Co-occurring native species using parametric and nonparametric classifiers. IEEE Trans. Geosci. Remote. Sens. 57. https://doi.org/10.1109/TGRS.2019.2902774.
Merzlyak, M.N., Gitelson, A.A., Chivkunova, O.B., Solovchenko, A.E., Pogosyan, S.I., 2003. Application of Reflectance Spectroscopy for Analysis of Higher Plant Pigments. Russ. J. Plant Physiol. 50, 704–710.
Metternicht, G., 2003. Vegetation indices derived from high-resolution airborne videography for precision crop management. Int. J. Remote Sens. 24, 2855–2877.
Morais, M.C., Freitas, H., 2015. Phenological dynamics of the invasive plant Acacia longifolia in Portugal. Weed Res. 55, 555–564.
Moyo, H.P.M., Fatunbi, A.O., 2010. Utilitarian perspective of the invasion of some South African biomes by Acacia mearnsii. Global J. Environ. Res. 4, 6–17.
Mucina, L., Rutherford, M.C., 2006. The vegetation of South Africa, Lesotho and Swaziland. South African National Biodiversity Institute.
Müllerová, J., Pergl, J., Pyšek, P., 2013. Remote sensing as a tool for monitoring plant invasions: testing the effects of data resolution and image classification approach on the detection of a model plant species Heracleum mantegazzianum (giant hogweed). Int. J. Appl. Earth Obs. Geoinf. 25, 55–65.
Müllerová, J., Brůna, J., Bartaloš, T., Dvořák, P., Vítková, M., Pyšek, P., 2017. Timing is important: unmanned aircraft vs. Satellite imagery in plant invasion monitoring. Front. Plant Sci. 8, 887.
Mutanga, O., Skidmore, A.K., 2004. Narrow band vegetation indices overcome the saturation problem in biomass estimation. Int. J. Remote Sens. 25, 3999–4014.
Naidoo, L., Cho, M.A., Mathieu, R., Asner, G., 2012. Classification of savanna tree species, in the Greater Kruger National Park region, by integrating hyperspectral and LiDAR data in a Random Forest data mining environment. ISPRS J. Photogramm. Remote. Sens. 69, 167–179.
Ollinger, S.V., 2011. Sources of variability in canopy reflectance and the convergent properties of plants. New Phytol. 189, 375–394.
Pedregosa, F., Varoquaux, G., Gramfort, A., Michel, V., Thirion, B., Grisel, O., Blondel, M., Prettenhofer, P., Weiss, R., Dubourg, V., 2011. Scikit-learn: machine learning in Python. J. Mach. Learn. Res. 12, 2825–2830.
Peñuelas, J., Baret, F., Filella, I., 1995. Semi-empirical indices to assess carotenoids/chlorophyll a ratio from leaf spectral reflectance. Photosynthetica 31 (2), 221–230.
Perry, M.T., 2017. Rasterstats.
Pyšek, P., Jarošík, V., Hulme, P.E., Pergl, J., Hejda, M., Schaffner, U., Vilà, M., 2012. A global assessment of invasive plant impacts on resident species, communities and ecosystems: the interaction of impact measures, invading species' traits and environment. Glob. Chang. Biol. 18, 1725–1737.
Richardson, D.M., Van Wilgen, B.W., 2004. Invasive Alien Plants in South Africa: How Well Do We Understand the Ecological Impacts?.
Rocchini, D., Luque, S., Pettorelli, N., Bastin, L., Doktor, D., Faedi, N., Feilhauer, H., Féret, J., Foody, G.M., Gavish, Y., 2018. Measuring β-diversity by remote sensing: a challenge for biodiversity monitoring. Methods Ecol. Evol. 9, 1787–1798.
Rondeaux, G., Steven, M., Baret, F., 1996. Optimization of soil-adjusted vegetation indices. Remote Sens. Environ. 55, 95–107.
Rouse, J.W., Haas, R.H., Schell, J.A., Deering, D.W., 1974. Monitoring vegetation systems in the great plains with ERTS. In: Freden, S.C., Mercanti, E.P., Becker, M.A. (Eds.), Third Earth Resources Technology Satellite-1 Symposium. NASA, Washington, DC, pp. 309–317.
Sanner, M.F., 1999. Python: a programming language for software integration and development. J. Mol. Graph. Model. 17, 57–61.
Schlerf, M., Atzberger, C., Hill, J., 2005. Remote Sensing of Forest Biophysical Variables Using HyMap Imaging Spectrometer Data.
Serrano, L., Ustin, S.L., Roberts, D.A., Gamon, J.A., Peñuelas, J., 2000. Deriving Water Content of Chaparral Vegetation from AVIRIS Data. Remote Sens. Environ. 74, 570–581.
Sims, D.A., Gamon, J.A., 2002. Relationships between leaf pigment content and spectral reflectance across a wide range of species, leaf structures and developmental stages. Remote Sens. Environ. 81, 337–354.
Skowronek, S., Ewald, M., Isermann, M., Van De Kerchove, R., Lenoir, J., Aerts, R., Warrie, J., Hattab, T., Honnay, O., Schmidtlein, S., 2017. Mapping an invasive bryophyte species using hyperspectral remote sensing data. Biol. Invasions 19, 239–254.
Somers, B., Asner, G.P., 2012. Hyperspectral time series analysis of native and invasive species in Hawaiian rainforests. Remote Sens. (Basel) 4, 2510–2529.
Somers, B., Asner, G.P., 2013a. Invasive species mapping in Hawaiian rainforests using multi-temporal Hyperion spaceborne imaging spectroscopy. IEEE J. Sel. Top. Appl. Earth Obs. Remote. Sens. 6, 351–359.
Somers, B., Asner, G.P., 2013b. Multi-temporal hyperspectral mixture analysis and feature selection for invasive species mapping in rainforests. Remote Sens. Environ. 136, 14–27.
Somodi, I., Čarni, A., Ribeiro, D., Podobnikar, T., 2012. Recognition of the invasive species Robinia pseudacacia from combined remote sensing and GIS sources. Biol. Conserv. 150, 59–67.
Tucker, C.J., 1979a. Monitoring corn and soybean crop development with hand-held radiometer spectral data. Remote Sens. Environ. 8, 237–248.
Tucker, C.J., 1979b. Red and photographic infrared linear combinations for monitoring vegetation. Remote Sens. Environ. 8, 127–150.
van Rensburg, J.J., 2017. Managing invasive alien plants on private land in the Western Cape: insights from vergelegen Estate. Managing Invasive Alien Plants on Private Land in the Western Cape: Insights from Vergelegen Estate.
van Wilgen, B.W., Wilson, J.R., 2018. The Status of Biological Invasions and Their Management in South Africa in 2017. South African National Biodiversity Institute, Kirstenbosch and DST-NRF Centre of Excellence for Invasion Biology, Stellenbosch, pp. 398.
Vila, M., Ibáñez, I., 2011. Plant invasions in the landscape. Landsc. Ecol. 26, 461–472.
Vogelmann, J.E., Rock, B.N., Moss, D.M., 1993. Red Edge Spectral Measurements From Sugar Maple Leaves.
Wolkovich, E.M., Cleland, E.E., 2011. The phenology of plant invasions: a community ecology perspective. Front. Ecol. Environ. 9, 287–294.
Yapi, T.S., O'Farrell, P.J., Dziba, L.E., Esler, K.J., 2018. Alien tree invasion into a South African montane grassland ecosystem: impact of Acacia species on rangeland condition and livestock carrying capacity. Int. J. Bio. Sci. Ecosys. Ser. Manag. 14, 105–116.